282–288 *Nucleic Acids Research, 1996, Vol. 24, No. 2*

Distamycin-induced inhibition of formation of a nucleoprotein complex between the terminase small subunit G*1*P and the non-encapsidated end (*pac*L site) of *Bacillus subtilis* bacteriophage SPP1

Sunghee Chai[1,2] and Juan C. Alonso[1,*]

[1]Centro Nacional de Biotecnología, CSIC, Campus Universidad Autónoma de Madrid, Cantoblanco, 28049 Madrid, Spain and [2]Max-Planck-Institut Für molekulare Genetik, Ihnestrasse 73, D-14195 Berlin, Germany

Received October 9, 1995; Revised and Accepted November 21, 1995

ABSTRACT

The small subunit of the *Bacillus subtilis* bacteriophage SPP1 terminase (G*1*P) forms a sequence-specific nucleoprotein complex with the SPP1 non-encapsidated end (*pac*L site) during initiation of DNA encapsidation. Gel mobility shift assay was used to study the G*1*P–*pac*L interaction. Distamycin, a minor groove binder that induces local distortion of the DNA, inhibits G*1*P–*pac*L complex formation. The competition of G*1*P with distamycin for DNA binding at the *pac*L site is independent of the order of addition of the reactants. Other minor groove binders, such as spermine or Hoechst 33258, which do not distort DNA, failed to compete with G*1*P for *pac*L DNA binding. Cationic metals, which generate a repertoire of DNA structures different from that caused by the minor groove binders, can partially reverse the distamycin-induced inhibition of G*1*P binding to *pac*L DNA. The major groove binder methyl green, which does not distort sequence-directed bending of *pac*L DNA, competes with G*1*P for binding at the *pac*L site. Our data suggest that the natural sequence-directed bend that exists within the *pac*L site is the architectural element that facilitates assembly of a nucleoprotein complex and hence initiation of DNA encapsidation by bacteriophage SPP1.

INTRODUCTION

Initiation of packaging of double-stranded viral DNA concatemers involves specific interaction of the prohead with virus DNA in a process mediated by a phage-encoded DNA recognition and cleavage (terminase) protein (reviewed in 1,2). The terminase enzymes described so far, which are hetero-oligomers composed of a small and a large subunit, do not have a significant level of sequence homology (reviewed in 1). The role of the terminase small subunit is to specifically recognize the packaging initiation site (*cos* or *pac*). It is thought that the small terminase subunit forms a nucleoprotein structure that helps to position the terminase large subunit at *cos* or *pac* (reviewed in 1).

The *Bacillus subtilis* bacteriophage SPP1 terminase enzyme is composed of a small (G*1*P) and a large (G*2*P) subunit which are the products of genes *1* and *2* respectively (3). G*1*P (estimated native molecular mass 190–210 kDa) is a three-domain protein (DNA binding and G*1*P–G*1*P and G*1*P–G*2*P interacting domains) (4,5). The N-terminal domain contacts DNA by a helix–turn–helix (HTH) motif, the central domain mediates the G*1*P–G*1*P contact, whereas an uncharacterized domain could mediate G*1*P–G*2*P hetero-oligomer formation. No apparent biological role can be assigned to the C-terminal region (5).

The SPP1 *pac* region can be subdivided into three discrete sites (*pac*L, *pac*C and *pac*R). The G*2*P cleavage site (*pac*C) is located between the *pac*L and *pac*R sites (3–7; Fig. 1). G*1*P binds co-operatively to the encapsidated (*pac*R) and non-encapsidated (*pac*L) DNA ends and holds the two binding sites together in a DNA loop (4). DNase I footprinting experiments indicate that each G*1*P binding site contains two discrete binding domains, termed box **a** in *pac*L and box **c** in *pac*R (4; see Fig. 1). The *pac*L and *pac*R sites are separated from each other by a stretch of 140 bp (4). The center-to-center distance of these two non-adjacent sites is ~204 bp (4; Fig. 1). The G*1*P recognition site at *pac*L is embedded in a sequence-directed DNA bend. The interaction of G*1*P with *pac*L DNA is observed only on one side of the double helix (4). The *pac*L site contains two directly repeated boxes (box **a**), which are located four helical turns away from each other (Fig. 1). G*1*P binding to *pac*L enhances DNA bending. Therefore, any interaction between G*1*P bound to *pac*L and G*1*P bound to *pac*R would give rise to a loop of 204 bp in length (or ~20 turns of the DNA helix) (4). DNA loop formation mediated by G*1*P could distort the DNA within the loop and hence alter the binding characteristics of G*2*P to its asymmetric target site (4). Additional evidence for DNA looping is provided by alternating DNase I-hypersensitive and DNase I-resistant sites in the complexed DNA, which appear with an approximate periodicity of 10 bp (see Fig. 1). To address the nature of the interaction between G*1*P and the *pac*L site and to elucidate the influence of intrinsic DNA bending on this reaction several groove binders (GBs) were employed.

* To whom correspondence should be addressed

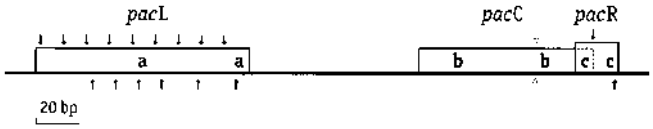

Figure 1. Schematic representation of the SPP1 *pac*L, *pac*C and *pac*R sites. The thick line indicates the SPP1 *pac* region. The open bars denote the non-encapsidated phage genome end (*pac*L), the packaging cleavage region (*pac*C) and the encapsidated end (*pac*R) respectively. The broken lines on the *pac*C bar denote the region of overlap. The directly repeated boxes **a**, **b** and **c** are depicted. The sites hypersensitive to DNase I digestion are denoted by vertical filled arrows. The vertical open arrows indicate the cleavage site at *pac*C. The distance in base pairs is indicated.

The pyrrole amide antibiotic distamycin A (henceforth distamycin) binds to the minor groove of B-DNA in a non-covalent and a non-intercalative mode (8). Distamycin associates preferentially with a nucleotide sequence rich in adenosine (A) and thymine (T) base pairs. Distamycin binds to the minor groove of B-DNA and induces local structural distortion by bending the DNA helix and inducing conformational changes in the neighborhood (9,10). Electron microscopic (11), ^{1}H-NMR (12) and X-ray crystallographic (13) studies provide direct evidence of distamycin-induced changes of local DNA structures. Distamycin interferes with proteins that act upon DNA binding (14–16). The binding of distamycin to the minor groove of DNA can compete with protein binding. Alternatively, the binding of distamycin in the minor groove induces a change in the local conformation which diminishes binding affinity of the protein for the major groove.

In this paper we present evidence that binding of G*1*P to the intrinsically bent locus within *pac*L is inhibited by the minor GB distamycin and the major GB methyl green. Distamycin competition for G*1*P binding to the *pac*L DNA segment is independent of the order of addition of the reactants. Other minor GBs that do not distort DNA upon binding (spermine and Hoechst 33258) do not compete with G*1*P for *pac*L binding. Cationic metals, which generate a different repertoire of DNA structures, can partially reverse the distamycin-induced inhibition of G*1*P binding to *pac*L DNA. It is likely, therefore, that the distamycin-induced conformational change diminishes the binding affinity of G*1*P for *pac*L DNA (the SPP1 non-encapsidated end).

MATERIALS AND METHODS

Bacterial strains and plasmids

Escherichia coli strain JM109 (17) and plasmid pBT397 (5) have been previously described.

Enzymes and reagents

SPP1 G*1*P was purified as previously described (5). Protein concentrations were determined by the method of Bradford (18), using bovine γ-globulin as a standard. The amount of G*1*P is expressed as mol protein protomers (predicted molecular mass of SPP1 G*1*P is 20.7 kDa). DNA restriction and modification enzymes and poly(dI-dC) were purchased from Boehringer Mannheim (Germany), distamycin and spermine from Sigma (USA), Hoechst 33258 from Polysciences Inc. (USA) and methyl green from ICN (Germany). All chemicals used were reagent grade and solutions were made in quartz-distilled H_2O.

[α-^{32}P]dATP was from Amersham Buchler GmbH (Germany). Ultra pure acrylamide was from Serva (Germany).

DNA manipulations

Covalently closed circular plasmid DNA was purified by the SDS lysis method (19), followed by purification on a cesium chloride–ethidium bromide gradient. Gel-purified DNA fragments were end-labeled by filling in the restriction site with the large fragment of DNA polymerase I in the presence of [α-^{32}P]dATP and dTTP, dCTP and dGTP.

Analytical and preparative gel electrophoresis of plasmid DNA and restriction fragments was carried out either in 0.8% (w/v) agarose, Tris–acetate–EDTA, ethidium bromide horizontal slab gels or 4% (w/v) non-denaturing polyacrylamide, Tris–borate gels (19).

The relative amounts of DNA present in any particular band in the autoradiograms was quantitatively scanned with a laser densitometer (LKB UltroScan XL). The linearity of the response with respect to DNA concentration was checked using autoradiograms at different exposure times. Quantitative scans were integrated using the LKB GelScan XL software package.

The concentration of the 324 bp *pac*L DNA was determined using molar extinction coefficients of 6500/M/cm at 260 nm. Except for poly(dI-dC), the amount of DNA is expressed as mol DNA molecules.

Gel shift assay

The SPP1 271 bp *Hpa*II–*Bsm*I SPP1 *pac*L DNA fragment (obtained as a 324 bp segment) was labeled with [α-^{32}P]dATP by filling in the ends (*Eco*RI–*Hin*dIII) with the large fragment (Klenow) of DNA polymerase I. The unincorporated nucleotides were removed by gel filtration.

In all conditions 23 pM α-^{32}P-labeled DNA (324 bp *pac*L DNA) and 1 µg poly(dI-dC) were used per reaction mixture (20 µl). When required the *pac*L DNA was incubated with an excess of G*1*P (240 nM) for 10 min at 37°C. When indicated increasing concentrations of a GB or metal cations were added prior to or after G*1*P–*pac*L complex formation. The binding reactions were immediately subjected to 4% non-denaturing polyacrylamide gel electrophoresis (ndPAGE) and run at 2 V/cm at 4°C. The gels were dried prior to autoradiography.

RESULTS

G*1*P binding to the *pac*L DNA is inhibited by distamycin

Recently it has been shown that: (i) the SPP1 terminase small subunit (G*1*P) binds specifically and co-operatively to *pac*L (non-encapsidated end) and *pac*R (encapsidated end) sites; (ii) the *pac*L site contains an intrinsically bent sequence; (iii) G*1*P binding to the *pac* region enhances DNA looping between the *pac*L and *pac*R sites (4). To address whether the intrinsically bent *pac*L sequence plays a role in G*1*P–*pac*L interaction we have analyzed the influence of distamycin on G*1*P binding by gel shift assay. It has been reported that at low doses (500 nM–1 µM) distamycin selectively prevents DNA bending and does not abolish protein–DNA interactions, whereas high doses (1–200 µM) induce local structural distortions by bending the DNA helix (9,10).

In a previous study we showed that G*1*P–*pac* DNA complexes remain in the well when a low ionic strength ndPAGE running

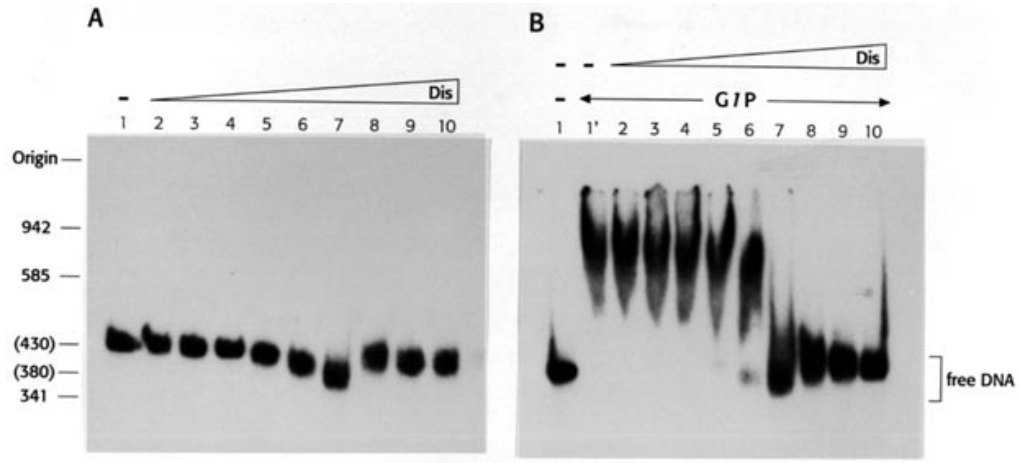

Figure 2. Effect of distamycin on *pac*L and on G*1*P–*pac*L DNA complex formation. (**A**) ^{32}P-Labeled 324 bp *pac*L DNA (23 pM) and 1 µg poly(dI-dC) were incubated with increasing concentrations of distamycin (Dis) for 20 min at room temperature (reaction mixture 20 µl) and then for 10 min at 37°C prior to 4% ndPAGE. (**B**) ^{32}P-Labeled 324 bp *pac*L DNA (23 pM) and 1 µg poly(dI-dC) were pre-incubated with increasing concentrations of distamycin for 20 min at room temperature before addition of G*1*P (240 nM). The reaction mixture (20 µl) was then incubated for 10 min at 37°C and subjected to 4% ndPAGE. Lanes 1 and 1′, DNA incubated without distamycin. Lanes 2–10, distamycin at: lane 2, 1 nM; lane 3, 10 nM; lane 4, 50 nM; lane 5, 100 nM; lane 6, 500 nM; lane 7, 1 µM; lane 8, 10 µM; lane 9, 50 µM; lane 10, 100 µM.

buffer is used in the gel shift assay, whereas in high ionic strength ndPAGE a diffuse retarded G*1*P–*pac* DNA complex is observed (5). Under high ionic strength ndPAGE conditions, however, an ~15-fold excess of G*1*P is required to saturate the DNA substrate when compared with the G*1*P–*pac* DNA complexes retained by the filter binding assay (see 4). Since a high ionic strength ndPAGE running buffer was used, we first set up the conditions of the gel shift assay to maximize complex formation using a fixed amount of labeled DNA fragment (23 pM) and purified G*1*P (240 nM).

The SPP1 324 bp [^{32}P]*pac*L DNA, which is rich in dA + dT, migrates much slower than a 430 bp size marker DNA fragment in 4% ndPAGE at 4°C (4; Fig. 2A). This anomalous mobility is greatly reduced at higher temperatures, implying the existence of sequence-directed curvature (see 4).

To examine the influence of distamycin on the conformation of *pac*L DNA we incubated the 324 bp [^{32}P]*pac*L DNA (23 pM) and 1 µg poly(dI-dC) with varying concentrations of distamycin (1 nM–100 µM) and subjected the reaction mixture to ndPAGE. As revealed in Figure 2A, distamycin influences the mobility of *pac*L DNA. Distamycin concentrations from 1 nM to 1 µM increase the mobility of the *pac*L DNA fragment. In the presence of 1 µM distamycin the 324 bp [^{32}P]*pac*L DNA segment migrated between the 341 and 380 bp size markers (‘reduced curvature’), but in the presence of higher concentrations of distamycin (5–100 µM) the DNA fragment again migrated slower than the 430 bp size marker DNA fragment (Fig. 2A).

In the presence of 100 nM distamycin (~13 distamycin molecules/bp *pac*L DNA) migration of the fragment was faster than in its absence, but to obtain the fastest migrating DNA segment 1 µM distamycin (134 distamycin molecules/bp *pac*L DNA) was needed. The absence of a large excess of non-specific competitor DNA [1 µg poly(dI-dC)] did not alter the pattern observed in Figure 2A (data not shown). It is likely, therefore, that poly(dI-dC) does not titrate distamycin for *pac*L DNA.

Pre-incubation of distamycin with the 324 bp [^{32}P]*pac*L DNA fragment (23 pM) reduced the ability of G*1*P (240 nM) to bind to its target DNA in a concentration-dependent manner (Fig. 2B). Inhibition of G*1*P binding to *pac*L DNA occurred at the same distamycin concentrations that modified or eliminated curvature of the naked DNA (Fig. 2A and B).

As revealed in Figure 2B, G*1*P–*pac*L DNA complex formation was completely blocked at 1 µM distamycin, while the first indication of inhibition of complex formation was seen at 500 nM distamycin. The amount of distamycin required to prevent 50% G*1*P–*pac*L DNA complex formation was ~750 nM. The distamycin-induced inhibition of G*1*P–*pac*L DNA complex formation is independent of the order of addition of the reactants. The same results were obtained when the *pac*L DNA was pre-incubated with distamycin and G*1*P was added subsequently as when the G*1*P–DNA complex was pre-formed and then challenged with distamycin (data not shown).

It could be hypothesized that distamycin inhibits G*1*P–*pac*L complex formation either by competing for binding to the minor groove of DNA or by altering the local DNA conformation of *pac*L DNA, which could diminish the binding affinity of G*1*P for DNA. These two possibilities were therefore analyzed.

The minor groove binders spermine and Hoechst 33258 do not compete with G*1*P for binding to *pac*L DNA

To analyze whether distamycin-induced inhibition of G*1*P binding to *pac*L DNA is due to an occupancy of the same site we used minor GBs that do not modify the structure of DNA upon binding, such as spermine (20) or Hoechst 33258 (21).

The presence of increasing concentrations of spermine (100 nM–1 mM) or Hoechst 33258 (100 nM–10 µM) did not alter the migration of DNA in 4% ndPAGE at 4°C (Fig. 3A and data not shown). The presence of concentrations of Hoechst 33258 >10 µM produced cross-linked or precipitated material and the DNA did not enter the gel.

Pre-incubation of *pac*L DNA (23 pM) and 1 µg poly(dI-dC) with increasing concentrations of spermine (100 nM–1 mM; Fig. 3B) or of Hoechst 33258 (100 nM–10 µM; data not shown) and

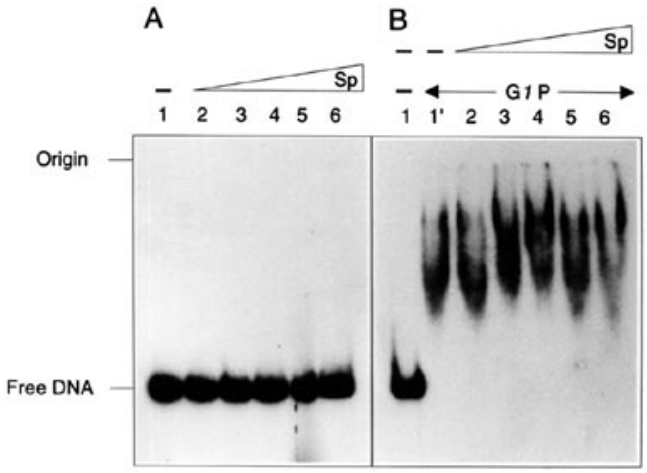

Figure 3. Effect of spermine on *pac*L and on G*1*P–*pac*L DNA complex formation. (**A**) ^{32}P-Labeled 324 bp *pac*L DNA (23 pM) and 1 µg poly(dI-dC) were incubated with increasing concentrations of spermine (sp) for 5 min at 37°C (reaction mixture 20 µl) and subjected to 4% ndPAGE. Lanes 2–6, spermine at: lane 2, 100 nM; lane 3, 1 µM; lane 4, 10 µM; lane 5, 100 µM; lane 6, 1 mM. (**B**) ^{32}P-Labeled 324 bp *pac*L DNA (23 pM) and 1 µg poly(dI-dC) were incubated with increasing concentrations of spermine as in (A) (lanes 2–6) before addition of G*1*P (240 nM). The reaction mixture (20 µl) was then incubated for 10 min at 37°C and subjected to 4% ndPAGE. Lanes 1 and 1′, DNA not treated with spermine.

subsequent addition of G*1*P (240 nM) did not affect the affinity of G*1*P for *pac*L DNA under our experimental conditions. The same effect was observed when pre-formed complexes of G*1*P–*pac*L DNA were challenged with increasing concentrations of spermine or Hoechst 33258 (data not shown). The presence of a large excess (up to 4×10^3 molecules) of spermine per G*1*P molecule did not affect its binding to *pac*L DNA. It seems, therefore, that the minor GBs spermine and Hoechst 33258 do not compete with G*1*P for binding to *pac*L DNA.

Cationic metals partially compete with G*1*P binding to *pac*L DNA

Certain divalent cationic metals, such as Ba^{2+}, Co^{2+}, Mn^{2+} and Zn^{2+}, can promote sequence-directed DNA bending (22). The fraction of molecules with a cation-induced bend is dependent on both the type and the concentration of cationic metal. $MnCl_2$ and $BaCl_2$ are most effective in inducing curvature at 50–100 mM and less effective at higher concentrations (22). To analyze whether cationic metals could affect G*1*P binding to *pac*L DNA by generating a different repertoire of bent structures we have used $BaCl_2$ and $MnCl_2$ (see 22).

As revealed in Figure 4, the addition of 40–160 mM $BaCl_2$ or $MnCl_2$ reduced the mobility of the intrinsically bent 324 bp [^{32}P]*pac*L (23 pM) DNA segment in 4% ndPAGE at 4°C, implying that curvature is increased in the presence of the divalent cations. In the presence of 160 mM $BaCl_2$ <3% of total DNA showed an anomalous mobility, but at the same concentration of $MnCl_2$ >99% of the molecules showed an anomalous mobility when compared with absence of the cationic metals (see Fig. 4).

Pre-incubation of *pac*L DNA (23 pM) and 1 µg poly(dI-dC) with increasing concentrations (5–40 mM) of $BaCl_2$ (Fig. 4A) or $MnCl_2$ (Fig. 4B) and subsequent addition of G*1*P (240 nM) did not affect the affinity of G*1*P for *pac*L DNA. It is likely, therefore,

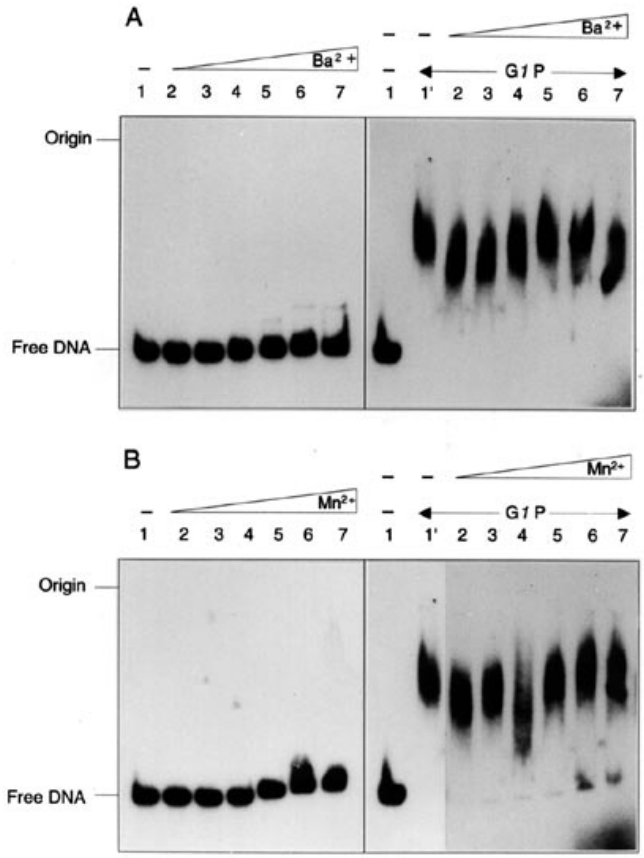

Figure 4. Effect of cationic metals on *pac*L DNA and on G*1*P–*pac*L DNA complex formation. (**A**) (Left) ^{32}P-Labeled 324 bp *pac*L DNA (23 pM) and 1 µg poly(dI-dC) were incubated with increasing concentrations of $BaCl_2$ (Ba^{2+}) for 5 min at 37°C (reaction mixture 20 µl) and subjected to 4% ndPAGE. Lanes 2–7, $BaCl_2$ at: lane 2, 5 µM; lane 3, 10 µM; lane 4, 20 µM; lane 5, 40 µM; lane 6, 80 µM; lane 7, 160 mM. (Right) the 324 bp [^{32}P]*pac*L DNA (23 pM) and 1 µg poly(dI-dC) were pre-incubated with increasing concentrations of $BaCl_2$ before addition of G*1*P (240 nM). The reaction mixture (20 µl) was then incubated for 10 min at 37°C. Lanes 1 and 1′, DNA not treated with $BaCl_2$. (**B**) (Left) ^{32}P-Labeled 324 bp *pac*L DNA (23 pM) and 1 µg poly(dI-dC) were pre-incubated with increasing concentrations of $MnCl_2$ (Mn^{2+}) for 10 min at 37°C (reaction mixture 20 µl). Lanes 2–7, $MnCl_2$ at: lane 2, 5 µM; lane 3, 10 µM; lane 4, 20 µM; lane 5, 40 µM; lane 6, 80 µM; lane 7, 160 mM. (Right) ^{32}P-Labeled 324 bp *pac*L DNA (23 pM) and 1 µg poly(dI-dC) were pre-incubated with increasing concentrations of $MnCl_2$ before addition of G*1*P (240 nM). The reaction mixture was then incubated for 10 min at 37°C and subjected to 4% ndPAGE. Lanes 1 and 1′, DNA not incubated with $MnCl_2$.

that the metal ions at concentrations ranging between 5 and 40 mM do not have a direct effect on G*1*P or on G*1*P interaction with DNA. In the presence of 80 or 160 mM $MnCl_2$, however, ~5% of total DNA were freed from the G*1*P–*pac*L complex (Fig. 4B). Similar results were observed when other cationic metals (e.g. $MgCl_2$) that induce sequence-directed DNA bending were used (data not shown). It is likely, therefore, that metal ion-induced bending (see Fig. 4A) can generate a DNA structure at *pac*L that is not recognized by G*1*P.

$BaCl_2$ reverses the distamycin-induced inhibition of G*1*P–DNA interaction

To examine whether distamycin-induced inhibition of G*1*P–*pac*L complex formation is due to a conformational change in the DNA

we pre-incubated the 324 bp *pac*L DNA with distamycin and with increasing concentrations of $BaCl_2$ or $MnCl_2$ prior to addition of G*1*P.

Figure 5A shows 324 bp [^{32}P]*pac*L DNA (23 pM) which was first incubated with 5 µM distamycin and then with increasing concentrations of $BaCl_2$. The latter reactant caused little effect, if any, on mobility of the DNA fragment in concentrations ranging from 5 to 20 mM. The presence of 40–160 mM $BaCl_2$ changed the mobility of 324 bp [^{32}P]*pac*L DNA (see Fig. 4A) and addition of distamycin enhanced such an effect (see Fig. 5A).

When the DNA was pre-incubated with 5 µM distamycin G*1*P was unable to form a complex with the 324 bp [^{32}P]*pac*L DNA (see Fig. 2B), whereas when the DNA was pre-incubated with 5 µM distamycin and 5–40 mM $BaCl_2$, G*1*P (240 nM) recovered its ability to bind the *pac*L DNA segment (Fig. 5B). The presence of $BaCl_2$ (20–40 mM) reversed the negative effect of distamycin on G*1*P–DNA complex formation and >70% of the DNA was complexed with G*1*P (Fig. 5B). At higher concentrations of $BaCl_2$ (80 mM) we did not observe reversal of distamycin-induced inhibition of the G*1*P–DNA interaction (Fig. 5B). Similar results were observed when $MnCl_2$ was used (data not shown). These results indicate that these metal ions at concentrations ranging between 5 and 40 mM enhance a specific structure(s) (‘active curvature’) on the DNA that reverses distamycin-induced inhibition of the G*1*P–DNA interaction, whereas other repertoires of structures fail to reverse the negative effect of distamycin on G*1*P binding to *pac*L DNA.

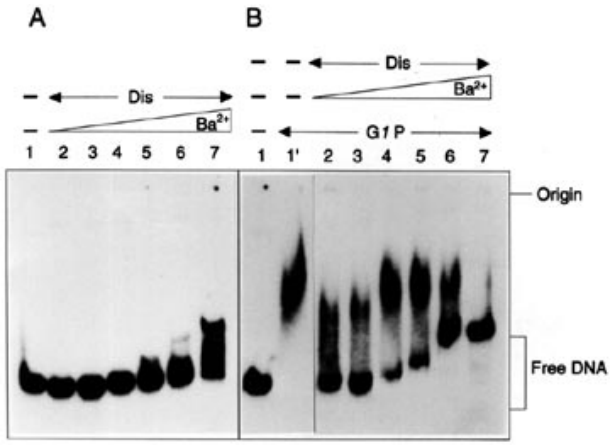

Figure 5. Effect of $BaCl_2$ on *pac*L and on G*1*P–*pac*L DNA complex formation. (**A**) ^{32}P-Labeled 324 bp *pac*L DNA (23 pM) and 1 µg poly(dI-dC) were pre-incubated with 5 µM distamycin for 20 min at room temperature. After subsequent addition of increasing concentrations of $BaCl_2$ (Ba^{2+}) for 10 min at 37°C (reaction mixture 20 µl) probes were subjected to 4% ndPAGE. Lanes 2–7, $BaCl_2$ at: lane 2, 5 mM; lane 3, 10 mM; lane 4, 20 mM; lane 5, 40 mM; lane 6, 80 mM; lane 7, 160 mM. (**B**) ^{32}P-Labeled 324 bp *pac*L DNA (23 pM) and 1 µg poly(dI-dC) were pre-incubated with 5 µM distamacyn for 20 min at room temperature and then with increasing concentrations of $BaCl_2$ as in (A) before addition of G*1*P (240 nM). The reaction mixture was then incubated for 10 min at 37°C and subjected to 4% ndPAGE. Lanes 1 and 1′, DNA not treated with $BaCl_2$.

Methyl green partially competes with G*1*P for binding to *pac*L DNA

In a previous study we showed that G*1*P lacking the DNA binding HTH motif (G*1*P*) is able to interact with wild-type G*1*P, but fails to bind to the SPP1 *pac* region (5). It is thought that the HTH motif is the principal structural element of the terminase small subunit of many different phages (reviewed in 1). To investigate whether G*1*P–*pac*L interaction also occurs in the major groove of DNA we measured G*1*P–DNA complex formation in the presence of increasing concentrations of methyl green, which is a major GB (see 23).

As revealed in Figure 6A, the addition of 50 nM–50 µM methyl green did not modify mobility of the intrinsically bent SPP1 324 bp [^{32}P]*pac*L (23 pM) DNA segment in 4% ndPAGE at 4°C.

Methyl green concentrations ranging from 50 nM to 1 µM did not alter the rate of G*1*P–DNA complex formation, but at 50 µM it decreased the DNA binding activity of G*1*P to *pac*L DNA (Fig. 6B). The amount of methyl green required to prevent 50%

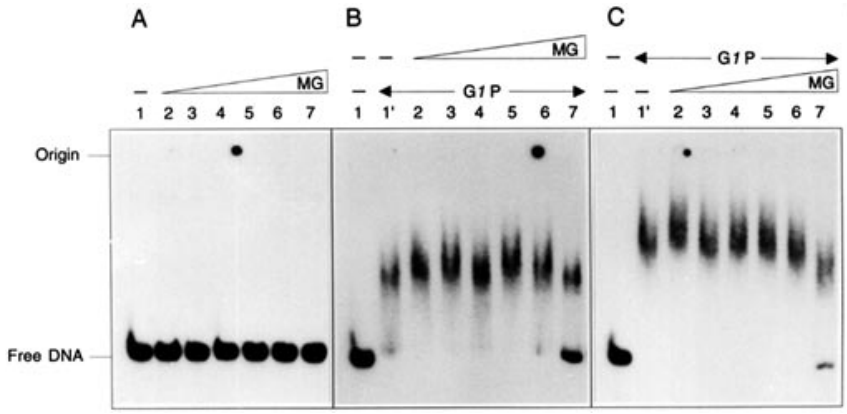

Figure 6. Effect of methyl green on *pac*L and on G*1*P–*pac*L DNA complex formation. (**A**) ^{32}P-Labeled 324 bp *pac*L DNA (23 pM) and 1 µg poly(dI-dC) were incubated with increasing concentrations of methyl green (MG) for 10 min at 37°C (reaction mixture 20 µl) and subjected to 4% ndPAGE. Lanes 2–7, methyl green at: lane 2, 50 nM; lane 3, 100 nM; lane 4, 500 nM; lane 5, 1 µM; lane 6, 10 µM; lane 7, 50 µM. (**B**) ^{32}P-Labeled 324 bp *pac*L DNA (23 pM) and 1 µg poly(dI-dC) were pre-incubated with increasing concentrations of methyl green as in (A) for 10 min at 37°C before addition of G*1*P (240 nM). The reaction mixture (20 µl) was then incubated for 10 min at 37°C. (**C**) ^{32}P-Labeled 324 bp *pac*L DNA (23 pM) and 1 µg poly(dI-dC) were pre-incubated with 240 nM G*1*P for 10 min at 37°C before addition of increasing concentrations of methyl green as in (A). Lanes 1 and 1′, DNA not treated with methyl green.

G*1*P–*pac*L DNA complex formation, compared with an untreated control, is <50 μM. Similar results were obtained when the *pac*L DNA was pre-incubated with methyl green and G*1*P was subsequently added (Fig. 6C; our unpublished results).

DISCUSSION

Genetic evidence suggests that the terminase enzyme from the *B.subtilis* phage SPP1 is essential for recognition and cleavage at the packaging initiation region (*pac*) (3). The terminase enzyme is a hetero-oligomer composed of a small (G*1*P) and a large (G*2*P) subunit, which are the products of genes *1* and *2* respectively. The *pac* region consists of three discrete sites (*pac*L, *pac*C and *pac*R) (4). The site of double-stranded DNA cleavage by G*2*P is called *pac*C (4,6,7), whereas the sites recognized by G*1*P in the encapsidated and non-encapsidated DNA strand are termed *pac*R (right) and *pac*L (left) respectively (4).

In previous studies we have shown that G*1*P is an oligomer (190–210 kDa) with a ring-like structure in solution. We have shown that several G*1*P molecules specifically interact with an intrinsically bent region of *pac*L covering a tract of almost 100 bp and that the specific interaction between G*1*P and *pac*L occurs on only one side of the DNA double helix (4). Upon binding to *pac* DNA G*1*P induces DNA bending and looping between the *pac*L and *pac*R sites and binding of G*1*P to *pac*L and *pac*R DNA facilitates assembly of a higher order nucleoprotein structure (4,5). On the basis of these data we have hypothesized that the G*1*P–*pac*L nucleoprotein complex and the G*1*P–*pac*R complex, with subsequent looping of the intervening DNA, could direct the positioning of G*2*P and define the directionality of DNA packaging (4).

The small subunit of the terminase enzyme from different bacteriophages interacts with DNA through a HTH DNA binding motif (1). In a previous study we postulated that G*1*P binding to the *pac* sites occurs in the major groove of B-DNA (3,5). In this study we show that methyl green, which is a major GB, affects the binding of G*1*P to *pac*L DNA. It is likely, therefore, that G*1*P interacts with DNA in the major groove.

The DNA features recognized by G*1*P indicate that the protein requires a bent DNA with an 'active' phase for assembly of a specialized nucleoprotein structure. Our studies have demonstrated that distamycin alters the mobility of *pac*L and interferes with G*1*P DNA binding. In the presence of 1 μM distamycin G*1*P fails to bind to the 'unbent' *pac*L DNA (Fig. 2B). Distamycin concentrations ranging from 5 to 100 μM, which decreased the mobility of *pac*L DNA, inhibit binding of G*1*P to ('distamycin-induced inactive bent') *pac*L DNA (Fig. 2B). Inhibition of G*1*P binding is also observed after addition of distamycin to preformed G*1*P–*pac*L DNA complexes, suggesting that either binding of the antibiotic to the minor groove can displace G*1*P from the DNA or that upon binding of distamycin in the minor groove it induces a conformational change in DNA which diminishes the binding affinity of G*1*P for *pac*L DNA. The competition of distamycin for G*1*P binding to *pac*L is neither the result of inhibition of contacts of G*1*P with the minor groove nor a direct interaction of distamycin and G*1*P that interferes with binding of the protein to *pac*L. These conclusions are based, first, on the findings that other minor GBs that do not affect the mobility of *pac*L DNA in ndPAGE do not affect G*1*P–*pac*L complex formation and, second, that metal ions, which are agents known to promote DNA bending, can partially reverse distamycin-induced inhibition.

Previous studies have demonstrated that distamycin interferes with the interaction of proteins that bind to the DNA major groove at concentrations comparable (1–2 μM) with those required to interfere with protein–DNA complex formation (24, this work) or greater (20–200 μM) (15). The interference caused by distamycin with proteins that interact with DNA through the major groove could be a result of a DNA conformation change, rather than a direct impediment due to occupancy by the minor GB of the protein target site. It is likely, therefore, that distamycin can effectively displace G*1*P bound in the major groove of DNA.

We show here that the specificity of G*1*P–*pac*L DNA binding is due not only to the sequence of its target site (box **a**), but also to the local conformation at that site. This conclusion is based on the finding that $BaCl_2$ and $MnCl_2$, which are agents known to promote DNA bending (22), can partially reverse (>70% of distamycin-induced inhibition at metal ion concentrations ranging from 20 to 40 mM) the inhibitory effect of distamycin. Higher concentrations of $BaCl_2$ or $MnCl_2$, which promote DNA looping, also exerted a negative effect on G*1*P–*pac*L complex formation. It is likely that only a limited repertoire of DNA structures promoted by the metal ions could reverse distamycin-induced inhibition of G*1*P–*pac*L complex formation.

The specific interaction of G*1*P with *pac*L occurs on only one face of the DNA double helix (4). It is likely that G*1*P deflects the *pac*L DNA towards itself upon binding and the net curvature of *pac*L reaches extremes when the deformation affects the same DNA face ('active bend') or opposite DNA faces ('inactive bend'). Distamycin could affect both DNA faces or the opposite DNA face, generating a different trajectory of the DNA path. It is likely, therefore, that distamycin inhibits G*1*P–*pac*L complex formation by altering the conformation of *pac*L DNA, rather than by competing for binding to the minor groove (see 9,16).

In summary, G*1*P seems to interact with *pac*L DNA via the major groove. Upon binding of G*1*P to box **a,** which is embedded in the intrinsically bent *pac*L DNA, ~100 bp are wrapped around a multimeric G*1*P molecule (4). Distamycin, which is a drug that has been shown to remove DNA curvature (9), inhibits G*1*P–*pac*L complex formation. DNA curvature, which is particularly pronounced in the presence of divalent cations, reverses distamycin-induced inhibition of G*1*P–*pac*L complex formation.

ACKNOWLEDGEMENTS

This work was partially supported by a grant from Dirección General de Investigación Cientifica y Técnica (PB93-0116) to JCA. We thank T.A.Trautner, F.Rojo and F.Weise for critical reading of the manuscript.

REFERENCES

1 Black,L.W. (1989) *Annu. Rev. Microbiol.*, **43**, 267–292.
2 Murialdo,H. (1991) *Annu. Rev. Biochem.*, **60**, 125–153.
3 Chai,S., Bravo,A., Lüder,G., Nedlin,A., Trautner,T.A. and Alonso,J.C. (1992) *J. Mol. Biol.*, **224**, 87–102.
4 Chai,S., Lurz,R. and Alonso,J.C. (1995) *J. Mol. Biol.*, **252**, 386–398.
5 Chai,S., Kruft,V. and Alonso,J.C. (1994) *Virology*, **202**, 930–939.
6 Bravo,A., Alonso,J.C. and Trautner,T.A. (1990) *Nucleic Acids Res.*, **18**, 2881–2886.
7 Deichelbohrer,I., Messer,W. and Trautner,T.A. (1982) *J. Virol.*, **42**, 83–90.
8 Zimmer,C. and Wahnert,U. (1986) *Prog. Biophys. Mol. Biol.*, **47**, 31–112.
9 Wu,H.-M. and Crothers,D.M. (1984) *Nature*, **308**, 509–513.

10 Kopka,M.L., Yoon,C., Goodsell,D., Pjura,P. and Dickerson,R.E. (1985) *Proc. Natl. Acad. Sci. USA*, **82**, 1376–1380.
11 Griffith,J., Bleyman,M., Rauch,C.A. Kitchin,P.A. and Englund,P.T. (1986) *Cell*, **46**, 717–724.
12 Klevit,R.R., Wemmer,D.E. and Reid,B.R. (1986) *Biochemistry*, **25**, 3296–3303.
13 Coll,M., Aymami,J., van der Marel,G.A., van Boom,J.H., Rich,A. and Wang,A.H.-J. (1989) *Biochemistry*, **28**, 310–320.
14 Bruzik,J.P., Auble,D.T. and deHaseth,P.L. (1987) *Biochemistry*, **26**, 950–956.
15 Broggini,M., Ponti,M., Ottlenghi,S., D'Incalci,M., Mongelli,N. and Mantovani,R. (1989) *Nucleic Acids Res.*, **17**, 1051–1059.
16 Straney,D.C. and Crothers,D.M. (1987) *Biochemistry*, **26**, 1987–1995.
17 Yanisch-Perron,C., Vieira,J. and Messing,J. (1985) *Gene*, **33**, 103–119.
18 Bradford,M.M. (1986) *Anal. Biochem.*, **72**, 248–254.
19 Sambrook,J., Maniatis,T. and Fritsch,E.F. (1989) *Molecular Cloning: A Laboratory Manual*, 2nd Ed. Cold Spring Harbor Laboratory Press, Cold Spring Harbor, NY.
20 Schmid,N. and Behr,J.-P. (1991) *Biochemistry*, **30**, 4357–4361.
21 Beerman,T.A., McHugh,M.M., Sigmund,R., Lown,J.W., Rao,K.E. and Bathini,Y. (1992) *Biochim. Biophys. Acta*, **1131**, 53–61.
22 Laundon,C.H. and Griffith,J.D. (1987) *Biochemistry*, **26**, 3759–3762.
23 Kumar,K.A. and Muniyappa,K. (1992) *J. Biol. Chem.*, **267**, 24824–24832.
24 Dorn,A., Affolter,M., Muller,M., Gehring,W.J. and Leupin,W. (1992) *EMBO J.*, **11**, 279–286.